EPR Studies of $S[M(CO)_5]_2^-$ Radicals (M = Cr, W) Trapped in Single Crystals of $PPN^+HS[M(CO)_5]_2^-$ †

Rosemary C. Hynes, Keith F. Preston,* Jerry J. Springs, and Antony J. Williams

Steacie Institute for Molecular Sciences, National Research Council of Canada, Ottawa, Ontario, Canada K1A 0R9

Received March 6, 1990

Persistent anisotropic EPR spectra detected in γ-irradiated single crystals of $PPN^+HSM_2(CO)_{10}^-$ (M = Cr, W) are attributed to the anion radicals produced by loss of a hydrogen atom from the undamaged anions. The **g** tensors were determined from measurements taken throughout three mutually orthogonal planes of crystallographically aligned single-crystal specimens: **g**(Cr) = (2.0008, 2.1142, 2.0472); **g**(W) = (1.9899, 2.2461, 2.0900). X-ray diffractometry showed that the undamaged crystals were isomorphous and belonged to the triclinic space group $P\bar{1}$. A full structure determination was carried out for the Cr compound only. Cell parameters for the Cr compound are as follows: a = 9.6629 (10) Å, b = 14.1626 (11) Å, c = 16.9509 (14) Å, α = 78.226 (7)°, β = 85.711 (8)°, γ = 89.615 (8)°, Z = 2. Cell parameters for the W compound are as follows: a = 9.825 (2) Å, b = 14.097 (4) Å, c = 17.019 (9) Å, α = 78.47 (3)°, β = 85.72 (3)°, γ = 89.91 (2)°. The anion structures showed an approximately octahedral arrangement of five carbonyls and a (shared) sulfur about each metal atom. Carbonyls from opposite ends of the anion are staggered with respect to each other. Cr–S bonds are 2.46 and 2.48 Å long and 122.8° apart. A good correlation was established for both Cr- and W-containing crystals between principal g values and the M–M direction (maximum g), the bisector of the M–S–M angle (intermediate g), and the perpendicular to the MSM plane (minimum g). These observations are interpreted in terms of a "π"-radical structure, analogous to that of SO_2^- in which unpaired spin density is shared between a S $3p_x$ orbital directed perpendicular to the CrSCr plane and Cr $3d_{xz}$ orbitals.

Introduction

Because of their implication in hydrodesulfurization catalysis[1,2] and in metalloprotein chemistry,[3-5] transition-metal thiolates have been studied closely. Research in this area has concentrated on synthesis and reactivity, with a natural focus on iron derivatives and iron–sulfur proteins. Group 6 thiolates have received increasing attention because of the involvement of iron–molybdenum–sulfur clusters in biochemical nitrogen fixation.[6] Very little effort has been directed toward the detection and characterization of free-radical intermediates in transition-metal thiolate chemistry. Some persistent 17-electron manganese and iron mercaptides are known,[7-9] and a claim[10] has been made for the radical $Cr(CO)_5SH$. In a very recent study of the oxidation chemistry of the binuclear thiolates $RS[Cr(CO)_5]_2^-$, the neutral free radicals $RS[Cr(CO)_5]_2$ have been characterized in liquid and frozen solution by EPR spectroscopy.[11] Somewhat surprisingly, the spectroscopic parameters for this type of radical indicate that the unpaired electron is located in a "π" semioccupied molecular orbital (SOMO) that has a dominant contribution from the S 3p atomic orbital directed perpendicular to the plane containing the sulfur and two metal atoms. As part of a program of study of bridged transition-metal carbonyl free radicals,[12-14] we decided to attempt a confirmation of this interesting result through studies of radiation-damaged single crystals of group 6 thiolates.

Experimental Section

(a) Preparation. $[PPN][HSCr_2(CO)_{10}]$ and $[PPN][HSW_2(CO)_{10}]$ were prepared according to established procedures.[15] Single crystals of these materials were grown from concentrated diethyl ether solutions at −20 °C by "layering" with n-pentane. Starting materials NaSH (Strem), [PPN]Cl (Aldrich), and $Cr(CO)_6$ (Strem) were used as received; solvents were purified by distillation from sodium–benzophenone ketyl or bought as reagent grade. Attempts to make single crystals of the molybdenum congener were unsuccessful.

† NRCC No. 32497.

Table I. Summary of X-ray Diffraction Data

compd	$[PPN][HSCr_2(CO)_{10}]$
formula	$C_{46}H_{31}NO_{10}P_2SCr_2$
fw	955.74
space group	$P\bar{1}$
cell params[a]	
a, Å	9.6629 (10)
b, Å	14.1626 (11)
c, Å	16.9509 (14)
α, deg	78.226 (7)
β, deg	85.711 (8)
γ, deg	89.615 (8)
V, Å^3	2264.5 (3)
Z	2
ρ_{calcd}, g cm^{-3}	1.402
cryst dimens, mm	0.20 × 0.20 × 0.20
temp, °C	24
radiation	Mo Kα
μ, cm^{-1}	6.4
data collection	ω–2θ
max, 2θ, deg	44.8
scan speed, deg min^{-1}	2
scan width, deg	1
total no. of observns	5803
no. of unique data, $I > 2.5\sigma(I)$	2779
final no. of variables	380
final max shift/error	0.569
max residual density, e/Å^3	1.050 (0.58 Å from Cr2)
secondary extinction coeff[b]	3.22 (17)
weighting scheme	unit weights
R[c] (signif data)	0.105
R_w[d] (signif data)	0.117
R[c] (all data)	0.1890
R_w[d] (all data)	0.1744
goodness of fit	0.75

[a] From 24 reflections in the 2θ range 30–40°. [b] Average path length in microns in a mosaic block. [c] $\sum||F_o| - |F_c||/\sum|F_o|$. [d] $[\sum w(|F_o| - |F_c|)^2/\sum wF_o^2]^{1/2}$.

(b) Crystallography. X-ray diffraction data (Table I) were collected for a crystal of the chromium compound on an Enraf-

(1) Weberg, R. T.; Haltiwanger, R. C.; Laurie, J. C. V.; Rakowski-Dubois, M. *J. Am. Chem. Soc.* **1986**, *108*, 6242.
(2) Harris, S.; Chianelli, R. R. *J. Catal.* **1984**, *86*, 400.

0276-7333/91/2310-0180$02.50/0 Published 1991 by the American Chemical Society

Table II. Atomic Parameters x, y, z and Temperature Factors B_{iso} for $PPN^+HSCr_2(CO)_{10}^-$[a,b]

	x	y	z	B_{iso}, Å^2
Cr1	0.9445 (3)	0.30976 (23)	0.15169 (19)	2.16 (14)
Cr2	1.3213 (3)	0.31916 (24)	0.27371 (20)	2.56 (14)
S	1.1784 (6)	0.3738 (5)	0.1575 (3)	8.1 (3)
O1	0.9999 (16)	0.2802 (11)	−0.0207 (9)	9.3 (9)
O2	0.8554 (17)	0.5113 (10)	0.0764 (9)	9.3 (10)
O3	0.6576 (15)	0.2338 (12)	0.1518 (11)	10.5 (11)
O4	0.8628 (20)	0.3428 (12)	0.3184 (9)	11.2 (12)
O5	1.0460 (20)	0.1061 (12)	0.2056 (12)	12.4 (12)
O6	1.3852 (20)	0.1447 (14)	0.2028 (15)	14.8 (15)
O7	1.1062 (16)	0.1937 (13)	0.3842 (10)	11.7 (11)
O8	1.5222 (18)	0.2680 (13)	0.3998 (11)	12.1 (11)
O9	1.2205 (23)	0.4835 (15)	0.3435 (12)	14.5 (15)
O10	1.5582 (15)	0.4461 (11)	0.1834 (9)	9.3 (9)
C1	0.9817 (19)	0.2919 (14)	0.0497 (14)	7.5 (12)
C2	0.8913 (22)	0.4351 (14)	0.1065 (13)	7.4 (12)
C3	0.7761 (24)	0.2635 (15)	0.1494 (13)	8.3 (12)
C4	0.8972 (22)	0.3274 (15)	0.2542 (13)	7.5 (12)
C5	1.0101 (23)	0.1890 (18)	0.1867 (15)	9.2 (14)
C6	1.3660 (22)	0.2176 (17)	0.2305 (15)	9.1 (14)
C7	1.1826 (22)	0.2431 (16)	0.3421 (14)	8.7 (13)
C8	1.4392 (23)	0.2886 (16)	0.3515 (16)	9.3 (14)
C9	1.262 (3)	0.410 (3)	0.3140 (18)	21.6 (27)
C10	1.4650 (20)	0.3956 (14)	0.2154 (12)	7.0 (11)
SH	1.225	0.434	0.102	8.6
P1	0.6287 (5)	0.8115 (3)	0.1617 (3)	4.86 (23)
P2	0.5266 (5)	0.8199 (3)	0.3279 (3)	4.94 (24)
N	0.5321 (14)	0.8410 (10)	0.2332 (7)	5.0 (7)
C11	0.5358 (17)	0.7305 (12)	0.1173 (10)	4.7 (4)
C12	0.4005 (18)	0.7046 (13)	0.1444 (11)	5.6 (4)
C13	0.3236 (20)	0.6442 (14)	0.1074 (12)	6.6 (5)
C14	0.3848 (20)	0.6100 (14)	0.0425 (12)	6.9 (5)
C15	0.5217 (21)	0.6348 (15)	0.0125 (12)	7.2 (5)
C16	0.6010 (19)	0.6932 (13)	0.0508 (11)	5.9 (4)
C21	0.6718 (17)	0.9177 (12)	0.0881 (10)	4.9 (4)
C22	0.7793 (22)	0.9115 (15)	0.0272 (13)	7.5 (5)
C23	0.8155 (24)	0.9971 (17)	−0.0325 (14)	8.7 (6)
C24	0.7438 (23)	1.0842 (16)	−0.0285 (14)	8.5 (6)
C25	0.6427 (21)	1.0861 (15)	0.0296 (12)	7.1 (5)
C26	0.6023 (19)	1.0034 (13)	0.0883 (11)	5.8 (4)
C31	0.7886 (17)	0.7564 (12)	0.1931 (10)	4.9 (4)
C32	0.8959 (20)	0.8164 (14)	0.2044 (12)	6.8 (5)
C33	1.0187 (23)	0.7741 (16)	0.2353 (14)	8.2 (6)
C34	1.0276 (22)	0.6728 (15)	0.2533 (13)	7.8 (5)
C35	0.9227 (21)	0.6170 (15)	0.2431 (12)	7.2 (5)
C36	0.8007 (19)	0.6562 (13)	0.2115 (11)	6.0 (4)
C41	0.6177 (16)	0.9113 (12)	0.3625 (10)	4.7 (4)
C42	0.6815 (21)	0.9868 (14)	0.3090 (12)	7.0 (5)
C43	0.7512 (25)	1.0606 (17)	0.3365 (15)	9.2 (6)
C44	0.7487 (25)	1.0562 (17)	0.4192 (15)	9.1 (6)
C45	0.6861 (23)	0.9792 (16)	0.4759 (13)	8.1 (6)
C46	0.6144 (21)	0.9056 (15)	0.4482 (13)	7.3 (5)
C51	0.3488 (17)	0.8291 (12)	0.3638 (10)	4.8 (4)
C52	0.2750 (20)	0.9090 (14)	0.3309 (12)	6.7 (5)
C53	0.1388 (22)	0.9203 (15)	0.3593 (13)	7.7 (5)
C54	0.0767 (22)	0.8517 (15)	0.4213 (13)	7.7 (5)
C55	0.1454 (22)	0.7731 (15)	0.4582 (13)	7.9 (6)
C56	0.2862 (20)	0.7580 (14)	0.4302 (12)	6.7 (5)
C61	0.5935 (18)	0.7052 (12)	0.3736 (10)	5.4 (4)
C62	0.7130 (20)	0.6958 (14)	0.4121 (12)	7.0 (5)
C63	0.7680 (24)	0.6045 (17)	0.4428 (14)	8.9 (6)
C64	0.6991 (24)	0.5240 (17)	0.4310 (14)	9.0 (6)
C65	0.5788 (23)	0.5301 (16)	0.3937 (14)	8.3 (6)
C66	0.5258 (20)	0.6234 (14)	0.3618 (12)	6.7 (5)

[a] Estimated standard deviations in parentheses refer to the last digit printed. [b] B_{iso} is the mean of the principal axes of the thermal ellipsoid.

Nonius CAD diffractometer controlled by NRCCAD software.[16] No higher symmetry or pseudosymmetry was found within a range of 3° when the cell reduction program CREDUC[16] was used. The linear absorption coefficient and crystal size (Table I) were such that absorption corrections were considered unnecessary. The structure was solved by direct methods, which gave most of the non-H atom positions; a difference Fourier analysis was used to locate the remaining atoms. Phenyl rings, including hydrogens, were included in the refinement as rigid groups, but the H atoms were not refined explicitly. The S–H hydrogen atom did not show up in the difference Fourier analysis; its position was calculated as 1.2 Å from the S in the SCr1Cr2 plane. Data reduction, structure solution, and refinement were all carried out with the NRCVAX system of crystal-structure programs.[17] The choice of 1.08 Å for C–H bonds in NRCVAX is based on past experience with the refinement of hydrocarbon structures. A scheme of unit weights gave the best refinement in terms of both R and R_w and the most reasonable bond lengths and angles; refinement with weights based on counting statistics gave less satisfactory results. A full listing of positional and thermal parameters for non-H atoms appears in Table II, and selected bond angles, distances, and directions are given in Table III. Complete listings of the structural data, including H atom parameters, are provided as

Table III. Selected[a] Bond Distances (Å) and Angles (deg) for $PPN^+HSCr_2(CO)_{10}^-$

	(a) Distances		
Cr1–S	2.457 (6)	S–SH	1.200 (6)
Cr1–C1	1.808 (24)	Cr1–C2	1.869 (20)
Cr1–C3	1.764 (25)	Cr1–C4	1.830 (21)
Cr1–C5	1.82 (3)	Cr2–S	2.481 (7)
Cr2–C6	1.780 (25)	Cr2–C7	1.891 (20)
Cr2–C8	1.79 (3)	Cr2–C9	1.65 (5)
Cr2–C10	1.859 (18)	P1–N	1.569 (13)
P2–N	1.569 (13)		
	(b) Angles		
Cr1–S–Cr2	122.79 (25)	Cr1–S–SH	118.6 (4)
Cr2–S–SH	118.6 (4)	S–Cr1–C1	92.6 (6)
S–Cr1–C2	88.0 (6)	S–Cr1–C3	179.0 (7)
S–Cr1–C4	90.2 (7)	S–Cr1–C5	88.8 (7)
C1–Cr1–C2	87.4 (9)	C1–Cr1–C3	88.4 (9)
C1–Cr1–C4	177.0 (9)	C1–Cr1–C5	87.6 (10)
C2–Cr1–C3	92.3 (9)	C2–Cr1–C4	91.8 (10)
C2–Cr1–C5	173.9 (18)	C3–Cr1–C4	88.8 (9)
C3–Cr1–C5	91.0 (10)	C4–Cr1–C5	93.3 (10)
S–Cr2–C6	87.1 (8)	S–Cr2–C7	97.0 (7)
S–Cr2–C8	173.6 (7)	S–Cr2–C9	89.6 (7)
S–Cr2–C10	87.9 (7)	C6–Cr2–C7	88.9 (10)
C6–Cr2–C8	93.7 (11)	C6–Cr2–C9	173.7 (10)
C6–Cr2–C10	93.9 (9)	C7–Cr2–C8	89.4 (10)
C7–Cr2–C9	86.2 (11)	C7–Cr2–C10	174.5 (10)
C8–Cr2–C9	90.2 (10)	C8–Cr2–C10	85.8 (9)
C9–Cr2–C10	91.3 (10)	P1–N–P2	136.5 (9)

[a] Full listing provided in the supplementary material.

(3) Coyl, C. L.; Zumft, W. G. In *Iron-Sulfur Protein Research*; Matsubara, H., Katsube, Y., Wada, K., Eds.; Japan Scientific Societies Press: Tokyo, 1987; pp 185–197.
(4) Berg, J. M.; Holm, R. H. In *Metal Ions in Biology*; Spiro, T., Ed.; Wiley: New York, 1982; pp 1–66.
(5) Holm, R. H. *Chem. Soc. Rev.* **1981**, *10*, 455.
(6) Cotton, F. A.; Wilkinson, G. *Advanced Inorganic Chemistry*, 5th ed.; Wiley: New York, 1988; Chapter 30.
(7) Treichel, P. M.; Molzahn, D. C.; Wagner, K. P. *J. Organomet. Chem.* **1979**, *174*, 191.
(8) Treichel, P. M.; Rosenhein, L. D. *Inorg. Chem.* **1984**, *23*, 4018.
(9) Winter, A.; Huttner, G.; Zsolnai, L.; Kroneck, P.; Gottlieb, M. *Angew. Chem., Int. Ed. Engl.* **1984**, *23*, 975.
(10) Behrens, V. H.; Linder, E.; Birkle, S. *Z. Anorg. Allg. Chem.* **1969**, 131.
(11) Springs, J.; Janzen, C. P., Darensbourg, M. Y.; Calabrese, J. C.; Krusic, P. J.; Verpeaux, J.-N.; Amatore, C. *J. Am. Chem. Soc.* **1990**, *112*, 5789.
(12) Morton, J. R.; Preston, K. F.; Le Page, Y.; Krusic, P. J. *J. Chem. Soc., Faraday Trans. 1* **1989**, *85*, 4019.
(13) Krusic, P. J.; Morton, J. R.; Preston, K. F.; Williams, A. J.; Lee, F. L. *Organometallics* **1990**, *9*, 697.
(14) Morton, J. R.; Preston, K. F.; Charland, J. P.; Krusic, P. J. *J. Mol. Struct.* **1990**, *223*, 115.
(15) Darensbourg, D. J.; Zalewski, D. J.; Sanchez, K. M.; Delord, T. *Inorg. Chem.* **1988**, *27*, 821.
(16) Le Page, Y.; White, P. S.; Gabe, E. J. *American Crystallographic Association Annual Meeting Abstracts*; Hamilton, Ontario, Canada, 1986; p 24.
(17) Gabe, E. J.; Lee, F. L.; Le Page, Y. *Crystallographic Computing 3*; Clarendon Press: Oxford, England, 1985; p 167.

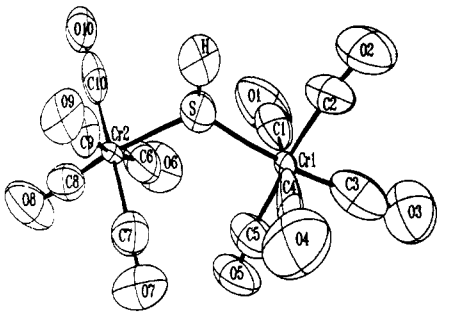

Figure 1. Structure of the undamaged $HSCr_2(CO)_{10}^-$ anion. Atom labeling as in Tables II and III.

supplementary material.

A comparison of unit cells for the Cr and W analogues showed that the two crystals were isomorphous; a crystal structure determination for $[PPN][HSW_2(CO)_{10}]$ was therefore deemed unnecessary. In the calculation of vectors within the crystal structure of the W congener, its measured unit cell parameters (a = 9.825 (2) Å, b = 14.097 (4) Å, c = 17.019 (9) Å, α = 78.47 (3)°, β = 85.72 (3)°, γ = 89.91 (2)°) were used, together with the fractional coordinates of the Cr congener. It was assumed, not unreasonably, that the fractional coordinates for the two congeners did not differ significantly.

Single crystals were irradiated at 77 K in a 400-TBq ^{60}Co source. The radicals generated were stable at room temperature for several days, enabling absolute alignment of the crystals on a Picker diffractometer according to the structural parameters. These crystals were glued inside the ends of 4-mm quartz tubes with one of the standard[18] orthogonal axes XYZ of the $P\bar{1}$ triclinic crystal aligned parallel to the length of the tube and with the direction of one of its other axes being indicated by a pointer attached to the tube. Contact of the crystals with air was minimized by coating them with epoxy glue in a drybox prior to alignment.

(c) EPR Spectroscopy. EPR spectra were obtained with a Varian Associates E-12 spectrometer. Magnetic field intensity was determined with a Bruker ER-035M gauss meter and microwave frequency with a Systron-Donner digital counter. With the quartz tube and affixed crystal placed in a liquid-nitrogen (77 K) dewar inside the microwave cavity of the spectrometer, the pointer lay over a horizontal brass protractor graduated every 5° of arc. By rotation of the tube about its long axis the magnetic field of the spectrometer could then explore a crystallographic plane. Three separate planes, XY, XZ, and YZ, were explored in order to characterize the triclinic unit cell.[19]

Results

Although the crystal structure of $[PPN][HSCr_2(CO)_{10}]$ had not been previously established, the structures of the individual ions were anticipated from X-ray diffraction studies on related materials.[20,21] The present structural data (Tables I–III) show that both ions have the expected geometries. (The unusually large spread in CO bond lengths in the anion is attributed to thermal motion.) The anion structure is of particular relevance to the EPR spectroscopic observations and is shown in Figure 1. Coordination about each Cr atom is very nearly octahedral, and the carbonyl ligands from opposite ends of the anion are staggered with respect to each other. The hydrogen atom (labeled SH in Table II and Figure 1) was assumed to lie in the SCr1Cr2 plane.

For an arbitrary orientation of the dc magnetic field, the EPR spectrum of a γ-irradiated single crystal of [PPN][$HSCr_2(CO)_{10}$] consisted of (Figure 2) a strong central resonance symmetrically flanked by two pairs of much weaker satellites. None of these resonances split upon rotation of the crystal, showing that site splitting[19] was absent, as expected for a triclinic system. The resonant magnetic field of the strong absorption was anisotropic, but the satellite pairs remained precisely centered about it for all orientations. The splitting ΔB, between the low-field and high-field components of each pair was very anisotropic, ranging in value between 0 and ≃90 G, and the components "crossed" for certain orientations. Such behavior is characteristic of the $\Delta m_S = \pm 1$ transitions in the crystal spectra of electronic triplets.[22] There was no evidence for the presence of resolved nuclear hyperfine interactions associated with any of the observed resonances in the crystal of $[PPN][HSCr_2(CO)_{10}]$. In the case of the tungsten-containing crystals, a single pair of weak satellite lines centered about the strong central resonance was detected for certain limited orientations (Figure 3). Their intensity relative to the central line, their separation, and its angular dependence were all suggestive of nuclear hyperfine interaction with a single tungsten nucleus in natural abundance (14.3% ^{183}W, $I = {}^1/_2$). Unfortunately, insufficient measurements of the interaction were available for determination of the associated tensor. The maximum ^{183}W hyperfine coupling observed was 40 G.

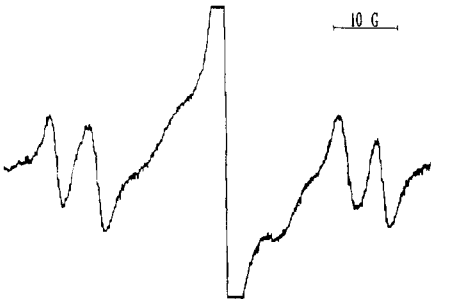

Figure 2. First-derivative EPR spectrum of a γ-irradiated single crystal of $[PPN][HSCr_2(CO)_{10}]$ at 77 K for the orientation B_0 = 30° from X in XY.

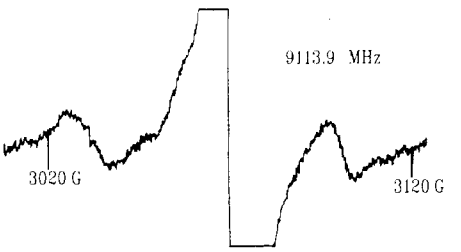

Figure 3. First-derivative EPR spectrum of a γ-irradiated single crystal of $[PPN][HSW_2(CO)_{10}]$ at 77 K, showing the ^{183}W satellites. The dc magnetic field lies 30° from Y in XY.

g^2 values were measured for the strong central resonances in irradiated $[PPN][HSCr_2(CO)_{10}]$ and $[PPN][HWCr_2(CO)_{10}]$ crystals and were plotted (see for example Figure 4) against angle for each crystal plane. The experimental data showed the expected[19] sinusoidal behavior. Matrix elements of the $\mathbf{g}^2$ tensors were obtained from[19] least-squares fits of expressions of the type

$$g^2(\theta) = g_{xx}^2 \cos^2\theta + g_{yy}^2 \sin^2\theta + g_{xy}^2 \sin 2\theta$$

to the experimental data. In the absence of site splitting, there was no ambiguity to be resolved in the relative signs

(18) Rollett, J. S. *Computing Methods in Crystallography*; Pergamon: Elmsford, NY, 1965; Chapter 3.
(19) Morton, J. R.; Preston, K. F. *J. Magn. Reson.* **1983**, *52*, 457.
(20) Handy, L. B.; Ruff, L. K.; Dahl, L. F. *J. Am. Chem. Soc.* **1970**, *92*, 7327.
(21) Cooper, M. K.; Duckworth, P. A.; Henrick, K.; McPartlin, M. *J. Chem. Soc., Dalton Trans.* **1981**, 2357.
(22) Wertz, J. E.; Bolton, J. R. *Electron Spin Resonance: Elementary Theory and Practical Applications*; McGraw-Hill: New York, 1972; Chapter 10.

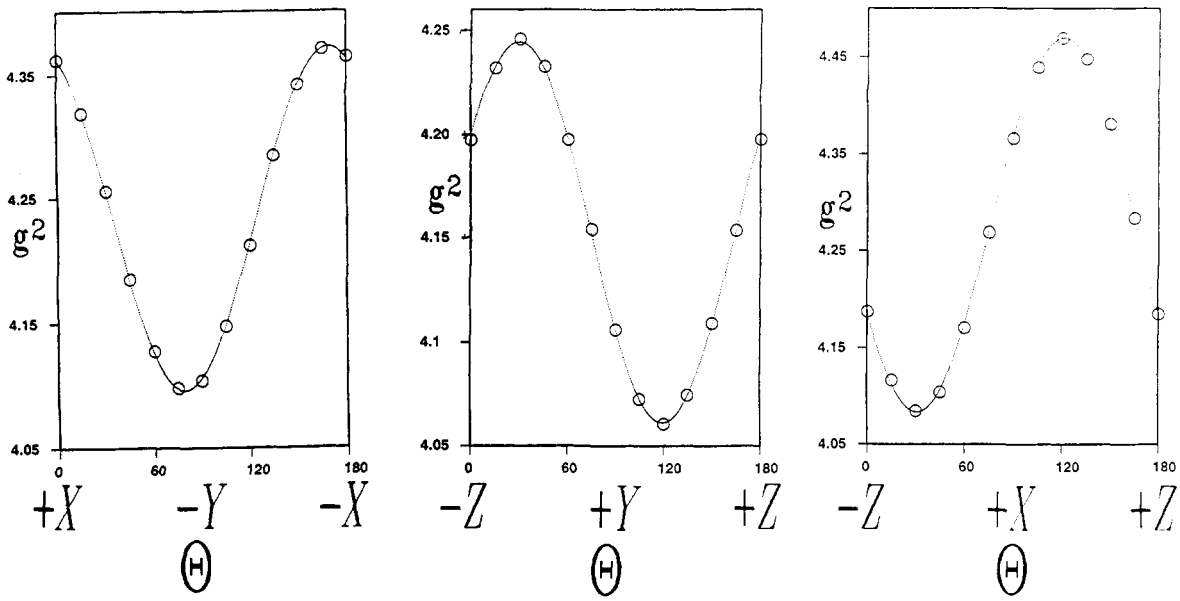

Figure 4. Plots of experimental values of g^2 against angles for the three orthogonal crystal planes and least-squares best-fit sinusoidal curves to the data.

Table IV. g^2 Tensors for the $SM_2(CO)_{10}^-$ Radicals (M = Cr, W) in Single Crystals of $PPN^+HSM_2(CO)_{10}^-$ at 77 K: Principal Values of *g* and Their Direction Cosines in the *XYZ* Axis System

	tensor			principal values and direction cosines of **g**		
	X	*Y*	*Z*	*x*	*y*	*z*
$\mathbf{g}^2$(Cr)				2.0008	2.1142	2.0472
	4.3636	0.0495	0.1714	0.3921	0.8498	−0.3522
	0.0495	4.1069	−0.0791	−0.6694	0.0010	−0.7429
	0.1714	−0.0791	4.1938	−0.6310	0.5271	0.5693
$\mathbf{g}^2$(W)				1.9899	2.2461	2.0900
	4.7236	0.1653	0.4387	0.4880	0.8179	−0.3047
	0.1653	4.2165	−0.1260	−0.6171	0.0764	−0.7832
	0.4387	−0.1260	4.4326	−0.6172	0.5703	0.5420

of the off-diagonal elements. The $\mathbf{g}^2$ tensors and their principal values and directions in the crystal *XYZ* basis are summarized in Table IV. A similar approach was adopted[23] in analyzing the satellite pairs in the Cr-containing crystal for the triplet fine-structure tensor, **D**. Plots of the scalar representation, $\beta g^3(\Delta B)/3$, of the matrix **g·D·g** against angle were obtained for each crystal plane from measurements of the separation, ΔB, of the $\Delta m_S = \pm 1$ components of each triplet. The best-fit tensor **g·D·g** was obtained by least-squares techniques[19,24] and was pre- and postmultiplied by $\mathbf{g}^{-1}$ to give **D** (Table V).

Discussion

The crystal structure shows the presence of two equivalent sites ($Z = 2$) that are related by inversion in the $P\bar{1}$ space group. It was therefore[19] no surprise to detect only one magnetic site for each of the paramagnetic entities observed by EPR spectroscopy. Since the impurity centers conform with the crystal symmetry, it is natural to assume that they are substitutional and to look for correlations of tensor principal directions with crystallographic directions in the undamaged ions. In both crystals there is, in fact, a striking correlation between the principal directions

Table V. g•D•g (MHz) Tensors for the Radical Pairs Observed in a $PPN^+HSCr_2(CO)_{10}^-$ Crystal: Principal Values of *D* (MHz) and Their Direction Cosines in the *XYZ* Crystal-Axis System

	tensor			principal values and direction cosines of **D**		
	X	*Y*	*Z*	*x*	*y*	*z*
g·D·g (A)				49.9	73.0	−124.6
	132.5	142.8	−222.7	0.8168	−0.4514	0.3593
	142.8	−23.4	349.8	0.5732	0.5638	−0.5947
	−222.7	349.8	−138.5	0.0659	0.6917	0.7192
	D = −186.9 MHz; E = −11.6 MHz					
g·D·g (B)				31.1	58.0	−88.7
	−378.0	66.1	5.0	0.0092	0.1090	0.9940
	66.1	226.1	20.6	0.2179	0.9699	−0.1083
	5.0	20.6	135.4	−0.9759	0.2176	−0.0149
	D = −133.1 MHz; E = −13.4 MHz					

Table VI. Correlation between Tensor Principal Directions and Directions within the Undamaged Anions[a]

radical	tensor component	angle to M1–M2	angle to bisector MSM	angle to perpendicular to MSM
$[Cr(CO)_5]_2S^-$	g_{min}	91.8	94.1	4.5
	g_{int}	90.1	4.2	85.9
	g_{max}	1.8	89.4	88.2
$[W(CO)_5]_2S^-$	g_{min}	86.7	97.8	8.5
	g_{int}	88.7	7.8	82.2
	g_{max}	3.5	90.2	93.4

[a] Angles in degrees.

of **g** and certain directions within the undamaged anions (Table VI). There can be little doubt, therefore, that the paramagnetic impurities derive from the host anions.

The lack of fine structure in the spectra and the proximity of the principal *g* values to that of a free spin (2.0023) lead us to conclude that the spectra have their origin with electronic doublets ($S = {}^1/_2$). Moreover, since the spectra show no resolved proton hyperfine structure, it is tempting to assign the radicals to the products of hydrogen atom loss from the parent anions, i.e. $[M(CO)_5]_2S^-$. The close correspondence of g_{min} with the perpendicular to the MSM plane, of g_{max} with the metal–metal direction, and of g_{inter} with the bisector of M–S–M (Table VI) strongly supports

(23) Pake, G. E.; Estle, T. L. *The Physical Principles of Electron Paramagnetic Resonance*; W. A. Benjamin: Reading, MA, 1973; Chapter 5.

(24) Morton, J. R.; Preston, K. F.; Darensbourg, M. Y. *Magn. Reson. Chem.* **1988**, *26*, 787.

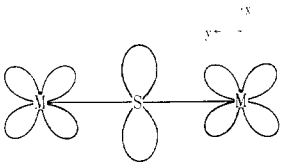

Figure 5. The "π" SOMO of $SCr_2(CO)_{10}^-$ and $SW_2(CO)_{10}^-$ shown in a projection along z.

this assignment: such an association is precisely what is expected for a free electron principally confined to a S $3p_x$ orbital directed perpendicular to the MSM plane (Figure 5). The situation is reminiscent of that in the prototypal free radical SO_2^- a 19-valence-electron species[25] with a well-established[26-28] π-SOMO (b_1 in C_{2v}) consisting of out-of-plane (x) p atomic orbitals on all three atoms. A dominant $3p_x$ contribution from the S atom, combined with that atom's large spin–orbit coupling constant, determines the departures of the g components of SO_2^- from the free-spin value. When B_0 is parallel to the $3p_x$ orbital, the principal g value is very close to the free-spin value; when B_0 lies along the O–O direction (y), spin–orbit interaction (between half-filled b_1 and filled a_1) is at a maximum and the g value is largest; with B_0 parallel to the 2-fold (z) axis, spin–orbit interaction is less efficient (with the filled b_2 level) but still results in a positive g shift and the intermediate principal g value. This alignment and ordering of the principal values of the tensor is paralleled by those in the radicals reported here.

As further support of our assignment, we note that the principal g values for the recently discovered[11] neutral radical $[Cr(CO)_5]_2SH$ are similar to those for the putative $[Cr(CO)_5]_2S^-$, although closer to the free-spin value: $g_{xx} = 2.0018$, $g_{yy} = 2.0471$, $g_{zz} = 2.0326$ (in THF/CH_2Cl_2). The slight reduction in g shifts as one passes from a free radical to its conjugate acid is quite normal and is due to the increased quenching of orbital angular momentum. Extended Hückel calculations support the contention[11] that radicals of the type $[Cr(CO)_5]_2SR$ have a π-type SOMO with a dominant contribution from S $3p_x$ and lesser contributions from Cr $3d_{xz}$ orbitals. Another parallel is to be found[29] in certain phosphinidene complexes that have a three-center π LUMO of composition similar to the SOMO of the radicals under discussion here. Our present **g**-tensor measurements are totally consistent with such an electronic structure and therefore favor assignments for the radicals in radiation-damaged $[PPN][HSM_2(CO)_{10}]$ to the conjugate bases $[M(CO)_5]_2S^-$.

Although we were unable to detect nuclear hyperfine satellites in the spectrum of the Cr compound or obtain spin densities from the sparse ^{183}W hyperfine interaction data, the **g** tensor (Table IV) points to some delocalization of the unpaired spin in the radicals. The increase in the shifts of the principal g values from the free-spin value on replacing Cr by W is a clear indication of the presence of unpaired spin in the metal orbitals. Tungsten has a spin–orbit coupling constant almost 1 order of magnitude larger than that of chromium,[30] so that an increase in g shifts is expected, provided some unpaired spin density is located in appropriate metal atomic orbital components of both the ground and excited states.

Table VII. Comparison of Experimental and Calculated Spin–Spin Interaction Tensors

site no.		d, Å[a]	$\lvert D\rvert$, $\lvert E\rvert$, MHz	direction cosines[b] X	Y	Z
1	exptl	6.93	186.9, 11.6	0.3593	−0.5947	0.7192
	calcd 1[c]		251.5, 2.8	0.5000	−0.5056	0.7031
	calcd 2[d]		184.9, 2.9	0.3071	−0.6251	0.7176
2	exptl	9.66	133.1, 13.4	0.9940	−0.1083	−0.0149
	calcd 1[c]		92.8, 0.6	0.9967	−0.0067	0.0811
	calcd 2[d]		111.4, 0.8	0.9996	−0.0232	−0.0181
3		8.21		0.7545	0.4195	−0.5047

[a] Distance between S atoms in symmetry-related anion sites. [b] Direction cosines of the maximum component fo the spin–spin tensor in the XYZ crystal axis system. [c] Calculated dipolar tensor and direction cosines for unit spin density on each S atom. [d] Calculated dipolar tensor and direction cosines for 46% spin on each S and 27% on each Cr atom.

The observation of triplet spectra associated with exchange-coupled pairs of neighboring radicals is now an established phenomenon in radiation-damaged metal hydrido carbonyls.[24,31] $[PPN][HSCr_2(CO)_{10}]$ certainly behaved normally in this respect, but disappointingly, the W congener gave no triplet spectra. The values and directions of the maximum spin–spin interaction for the two triplet species (Table V) correspond well with those calculated for dipolar interaction in two radical pairs formed from neighboring anion sites in the undamaged crystal (Table VII). Examination of the crystal structure reveals the presence of three close-neighbor anions with S–S distances of 6.92, 8.21, and 9.66 Å, but only the first and the last of these correlate well with the observed fine-structure tensors. This detection of a limited number of radical pairs parallels earlier observations[14,24,31] for radiation-damaged metal hydrido carbonyls. It is tempting, of course, to conclude that only certain radical pairs are formed by elimination of H_2. An alternative, however, is that *all* possible radical pairs are present but that superexchange occurs for certain combinations only; if the component radicals in the remaining pairs do not "see" each other, i.e. electron exchange does not take place ($J = 0$), they will exhibit the doublet ($S = {}^1/_2$) EPR spectrum of isolated radicals. Our studies[24] of radical pairs in $[PPN][HCr(CO)_5]$, where signals from electronic doublets were extremely weak, seem to mitigate against this alternative explanation.

Dipolar tensors for the radical pairs were taken[32] as the anisotropic part of the tensor

$$\tfrac{1}{2}\beta\sum_{i,j}\rho_i\rho_j r_{ij}^{-3}[\mathbf{g}\cdot\mathbf{g} - 3(\mathbf{g}\cdot\mathbf{r}) \wedge (\mathbf{g}\cdot\mathbf{r})]$$

where β is the Bohr magneton and ρ_i and ρ_j are the unpaired spin densities on atoms separated by the distance r_{ij} along the direction **r**. Calculations (Table VII) were carried out (1) for spin on the sulfur atom only and (2) for a distribution of 46% spin on each S and 27% on each Cr atom, which corresponds to the SOMO calculated by the extended Hückel method[11] for the protonated radical. Agreement with the observed tensor was better for the more realistic unpaired spin distribution; in particular, the principal directions for the maximum component of the tensors were within 4° of the experimental values. In both cases, however, the observed tensor was distinctly more

(25) Atkins, P. W.; Symons, M. C. R. *The Structure of Inorganic Radicals*; Elsevier: Amsterdam, 1967; Chapter 7.
(26) Schneider, J.; Dischler, B.; Räuber, A. *Phys. Status Solidi* **1966**, *13*, 141.
(27) Reuveni, A.; Luz, Z.; Silver, B. L. *J. Chem. Phys.* **1970**, *53*, 4619.
(28) Adrian, F. J.; Cochran, E. L.; Bowers, V. A. *J. Chem. Phys.* **1973**, *59*, 56.
(29) Huttner, G.; Evertz, K. *Acc. Chem. Res.* **1986**, *19*, 406.
(30) Goodman, B. A.; Raynor, J. B. *Adv. Inorg. Chem. Radiochem.* **1970**, *13*, 136.
(31) Krusic, P. J.; Morton, J. R.; Preston, K. F.; Le Page, Y. *J. Mol. Struct.* **1988**, *189*, 1.
(32) Abragam, A.; Bleaney, B. *Electron Paramagnetic Resonance of Transition Ions*; Clarendon Press: Oxford, England, 1970; p 492.

rhombic than that calculated. This discrepancy cannot be attributed to the anisotropy in **g**, which is allowed for in the above expression. Moreover, alternative spin distributions in which unpaired spin was spread over the carbonyl ligands led to smaller, rather than larger, values of E. We conclude that there must be a substantial spin-orbit contribution to the fine-structure tensor **D**. A similar situation arose for radical pairs of $Fe(CO)_4^-$ detected[31] in single crystals of $[PPN][HFe(CO)_4]$, where the tensors were markedly nonaxial and experimental D values were in considerable excess of the purely dipolar contribution. Unfortunately, it is not possible to estimate the importance of spin-orbit contributions to **D** without knowledge of the singlet-triplet energy gap in the excited states which connect to the ground singlet and triplet states via spin-orbit coupling.[31]

Conclusions

Analysis of the **g** tensors for the free-radical products of γ-irradiation of $[PPN][HSM_2(CO)_{10}]$ (M = Cr, W) leads to assignments to the radical anions arising from hydrogen atom loss. The molecular orbital occupied by the single unpaired electron in these species resembles that in SO_2^-: it has an important component from the S $3p_x$ orbital that is directed perpendicular to the plane containing the sulfur and metal atoms and smaller components from metal 3d orbitals. Weak satellite spectra present in the radiation-damaged Cr-containing compound are due to pairs of radicals (S = 1) located in certain nearest-neighbor sites.

Acknowledgment. We are indebted to R. Dutrisac of these laboratories for technical assistance.

Registry No. $[PPN][HSCr_2(CO)_{10}]$, 77310-17-9; $[PPN][HSW_2(CO)_{10}]$, 112680-81-6; $[Cr(CO)_5]_2S^-$, 130011-53-9; $[W(CO_5]_2S^-$, 130011-54-0.

Supplementary Material Available: Full tables of bond distances and angles, anisotropic thermal parameters, and positional parameters of hydrogen atoms for $[PPN][HSCr_2(CO)_{10}]$ (4 pages); a table of structure factors (30 pages). Ordering information is given on any current masthead page.

Synthesis and Crystal Structure of $[PPh_4]_2[Ir_4(CO)_{10}(CH_2COOMe)_2]$ and $[PPh_4][Ir_4(CO)_{11}(CH_2COOMe)]$. First Examples of Iridium Clusters Bearing an Alkyl-like Ligand

Fabio Ragaini and Francesca Porta*

Dipartimento di Chimica Inorganica e Metallorganica and CNR Center, v. Venezian 21, 20133 Milano, Italy

Francesco Demartin*

Istituto di Chimica Strutturistica Inorganica and CNR Center, v. Venezian 21, 20133 Milano, Italy

Received February 9, 1990

The reaction of $Na[Ir(CO)_4]$ ([Na]1) with given amounts of $BrCH_2COOMe$ in THF, followed by treatment with PPh_4Cl, gave high yields of the two novel clusters $[PPh_4]_2[Ir_4(CO)_{10}(CH_2COOMe)_2]$ ($[PPh_4]_2$**2**) and $[PPh_4][Ir_4(CO)_{11}(CH_2COOMe)]$ ($[PPh_4]$**3**). The reaction takes place in two steps; the first compound formed is **2**, which then reacts, in a slower reaction, with excess $BrCH_2COOMe$ to afford **3**. To the best of our knowledge, **2** and **3** are among the first examples of clusters bearing an alkyl or alkyl-like substituent. X-ray diffraction analysis of the clusters was carried out on crystals obtained by using PPh_4^+ as a countercation. Compound $[PPh_4]_2$**2** is triclinic, space group $P\bar{1}$, with a = 11.163 (2) Å, b = 12.807 (2) Å, c = 22.849 (3) Å, α = 84.76 (1)°, β = 88.76 (1)°, γ = 73.53 (1)°, Z = 2, R = 0.034, and R_w = 0.042 for 6373 independent reflections with $I > 3\sigma(I)$. Compound $[PPh_4]$**3** is monoclinic, space group $P2_1/c$, with a = 13.155 (4) Å, b = 24.593 (5) Å, c = 38.401 (8) Å, β = 91.00 (3)°, Z = 12, R = 0.065, and R_w = 0.069 for 5227 independent reflections with $I > 3\sigma(I)$. Both anions contain a tetrahedron of iridium atoms with three bridging CO ligands around a triangular basal face of the metal tetrahedron, the alkyl-like substituents being axially bonded to the iridium atoms of this face. The reactivity of the sodium salt of $[Ir(CO)_4]^-$ with $BrCH_2COOMe$ was quite different from that, already reported by us, of the same anion with PPN^+ ($PPN^+ = (PPh_3)_2N^+$) as a countercation. This latter reaction forms only mononuclear species. The possible role of Na^+ in the formation of the clusters is discussed.

Introduction

It has often been claimed that cluster compounds are possible models for heterogeneous catalysis and have even been proposed as homogeneous catalysts themselves.[1] Metal-alkyl species are often supposed to form at the active metal sites in many heterogeneously catalyzed reactions, but, to the best of our knowledge, only a few osmium or rhenium clusters bearing alkyl or alkyl-like ligands have been reported,[2] although many clusters with μ-carbene or carbyne groups are known.

(1) Gates, B. C., Guczi, L., Knozinger, H., Eds.; *Metal Clusters in Catalysis*; Studies in Surface Science and Catalysis 29; Elsevier: Amsterdam, 1986.

(2) (a) Zoet, R.; van Koten, G.; Vrieze, K.; Jansen, J.; Goubits, K.; Stam, C. H. *Organometallics* **1988**, *7*, 1565. (b) Bassner, S. L.; Morrison, E. D.; Geoffroy, G.; Rheingold, A. *Organometallics* **1987**, *6*, 2207. (c) Zuffa, J. L.; Gladfelter, W. L. *J. Am. Chem. Soc.* **1986**, *108*, 4669. (d) Morrison, E. D.; Bassner, S. L.; Geoffroy, G. L. *Organometallics* **1986**, *5*, 408. (e) Cree-Uchiyama, M.; Shapley, J. R.; St. George, G. M. *J. Am. Chem. Soc.* **1986**, *108*, 1316. (f) Churchill, M. R.; Lashewycz, R. A. *Inorg. Chem.* **1978**, *17*, 1291. (g) Masters, A. F.; Mertis, K.; Gibson, J. F.; Wilkinson, G. *Nouv. J. Chim.* **1977**, *1*, 389. (h) Edwards, P. G.; Felix, F.; Mertis, K.; Wilkinson, G. *J. Chem. Soc., Dalton Trans.* **1979**, 361. (i) Hursthouse, M. B.; Malik, K. M. A. *J. Chem. Soc., Dalton Trans.* **1978**, 1334. (j) A $\sigma + \pi$ alkenyliridium cluster has also been reported: Pierpont, C. G. *Inorg. Chem.* **1979**, *18*, 2972.

0276-7333/91/2310-0185$02.50/0